JCTC Journal of Chemical Theory and Computation

Article

pubs.acs.org/JCTC

Relative Free Energies for Hydration of Monovalent Ions from QM and QM/MM Simulations

Bogdan Lev,[†,§] Benoît Roux,*[,‡] and Sergei Yu. Noskov*[,†]

[†]Institute for Biocomplexity and Informatics, Department of Biological Sciences, The University of Calgary, 2500 University Drive, Calgary, Alberta, Canada T2N 1N4

[‡]Department of Biochemistry and Molecular Biology, Gordon Center for Integrative Sciences, The University of Chicago, 929 East 57th Street, Chicago, Illinois 60637, United States of America

ABSTRACT: Methods directly evaluating the hydration structure and thermodynamics of physiologically relevant cations (Na^+, K^+, Cl^-, etc.) have wide ranging applications in the fields of inorganic, physical, and biological chemistry. All-atom simulations based on accurate potential energy surfaces appear to offer a viable option for assessing the chemistry of ion solvation. Although MD and free energy simulations of ion solvation with classical force fields have proven their usefulness, a number of challenges still remain. One of them is the difficulty of force field benchmarking and validation against structural and thermodynamic data obtained for a condensed phase. Hybrid quantum mechanical/molecular mechanical (QM/MM) models combined with sampling algorithms have the potential to provide an accurate solvation model and to incorporate the effects from the surrounding, which is often missing in gas-phase *ab initio* computations. Herein, we report the results from QM/MM free energy simulations of Na^+/K^+ and Cl^-/Br^- hydration where we simultaneously characterized the relative thermodynamics of ion solvation and changes in the solvation structure. The Flexible Inner Region Ensemble Separator (FIRES) method was used to impose a spatial separation between QM region and the outer sphere of solvent molecules treated with the CHARMM27 force field. FEP calculations based on QM/MM simulations utilizing the CHARMM/deMon2k interface were performed with different basis set combinations for K^+/Na^+ and Cl^-/Br^- perturbations to establish the dependence of the computed free energies on the basis set level. The dependence of the computed relative free energies on the size of the QM and MM regions is discussed. The current methodology offers an accurate description of structural and thermodynamic aspects of the hydration of alkali and halide ions in neat solvents and can be used to obtain thermodynamic data on ion solvation in condensed phase along with underlying structural properties of the ion−solvent system.

I. INTRODUCTION

The theoretical and experimental studies of aqueous and nonaqueous electrolyte solutions form foundations of modern physical chemistry.[1] Studies of molecular interactions between ion and a solvent and ion-induced solvent reorganization processes are central for understanding of specific solvation phenomena.[2] While there have been extensive experimental and computational studies on the hydration of monovalent and polyvalent ions, a definitive picture of how these ions are solvated in water and to what extent structural differences in the organization of the solvation shell translate into differences in solvation thermodynamics is still lacking.[3] A molecular level understanding of the structural and thermodynamic features of specific ion ligation by organic molecule may potentially facilitate the design and fabrication of pores with programmed selectivity for use in areas ranging from water desalination[4,5] to molecular design of nanobatteries based on ion channels.[6] To elucidate the mechanisms that control the different interactions between an ion and a host, it may be helpful to accurately evaluate thermodynamic properties of a system, such as free energy of ion partitioning as well as structural features including the instantaneous and average coordination shell of the ion.

Simulations of complex systems are essentially limited by two main factors: the accuracy of the potential energy surface and the extent of statistical sampling.[7] Most simulations of ion solvation are based on molecular mechanical (MM) potential functions with fixed effective atomic charges,[8−10] which account implicitly for polarization effects. While this approximation allows fairly extensive simulations,[11] it is believed that classical MM force field may fail to correctly reproduce structural and thermodynamic properties due to the neglect of induced electronic polarization.[12] In particular, it was suggested that subtle differences in the coordination structure of Na^+ and K^+, which are two of the most prevalent ions in biology, might play an important role in the high selectivity required for the function of ion channels,[3,12] pumps,[13] and transporters.[3,14,15] One promising strategy to improve the accuracy of MD studies is the development of potential functions that explicitly account for induced polarization.[16−20] For example, such polarizable force fields have already provided some insight on water−ethanol mixtures,[21] hydrophobic hydration,[22] and membrane transport,[23] as well as ion solvation in water[20,24] and in liquid amides.[25] An important lesson learned while developing polarizable force fields is that detailed understanding of electronic effects in condensed phase is essential to develop accurately parametrized models.

One route for acquiring direct information about ion solvation that is free of the assumptions underlying classical force fields is to use *ab initio* quantum mechanical (QM)

Received: April 11, 2013
Published: August 5, 2013

   dx.doi.org/10.1021/ct400296w | *J. Chem. Theory Comput.* 2013, 9, 4165−4175

approaches.[26,27] *Ab initio* molecular dynamics (AIMD) simulations based on Density Functional Theory (DFT) methods have been applied with considerable success to studies of the structural features of aqueous solutions.[19,28−32] While the time scale afforded by such all-QM Carr−Parinello or Born−Oppenheimer MD simulations is typically on the order of tens of picoseconds, it is sufficient to characterize structural features of the hydrated ion, such as the coordination number, position of the first and second peaks in the radial distribution function (RDF) and extent of the first coordination shell.[19,33,34] The structural information obtained from AIMD simulations is in excellent agreement with the results obtained from X-ray and neutron diffraction as well as extended X-ray absorption fine structure (EXAFS) studies.[35] Leung and collaborators reported AIMD simulations for the estimation of the intrinsic solvation free energies for monovalent cations.[30,36] An important limitation of AIMD studies is the relatively small system size that can be simulated.[37] Avoiding finite-size effects in AIMD simulations is essential for a correct description of structural and thermodynamic properties.[38,39]

A natural route to reduce the computational burden of all-QM simulations and avoid the finite-size effects is to separate the full system into a moderately sized QM region and a large classical MM region. Such hybrid QM/MM methodology has been used to study enzymatic redox[40,41] reactions, proton transport,[42,43] hydroxylation,[44] and methylation.[45] Significant efforts have been made to enable free energy perturbation (FEP) methodologies from QM/MM simulations.[43,44,46−51] However, while there have been several applications of FEP combined with QM/MM simulations in studies of enzymes, its application to study the thermodynamics of ion solvation remains scarce.

There are primarily two challenges to carry out FEP calculations of ion solvation in bulk liquid based on QM/MM simulations. The first challenge lies in the treatment of a hybrid QM/MM system in which identical solvent molecules, which are rapidly diffusing and interchanging their positions, must be represented either at the QM or MM level depending on their position relative to the ion. This leads to a problem that is not encountered in QM/MM treatment of macromolecules, where a stable set of atoms is typically selected and assigned as the QM region for the entire duration of the simulation. To treat the problem of exchanges of QM water molecules with MM water molecules, we adopt the Flexible Inner Region Ensemble Separator (FIRES) partitioning scheme recently introduced by Rowley and Roux.[52] FIRES rigorously provides a dynamical and deformable separation between QM and MM regions in the FEP studies of ion hydration, which allows for a smooth integration along the FEP perturbation path and dynamical restructuring of solvent shell around an ion. The second challenge concerns the configurational sampling along the alchemical thermodynamic coupling parameter. Sampling is always a concern for any FEP calculations, though the problem may be more acute in the case of ion solvation due to the magnitude of the interactions involved and the considerable fluctuations that are inherent to a bulk solvent. While it is relatively easy to simply increase the length of trajectories in the case of classical force field simulations, this naïve approach is not practical in the case of QM/MM simulations. To circumvent the sampling issue, we adopted a Hamiltonian replica-exchange molecule dynamics (H-REMD) simulation methodology.

Our goal is to implement and test the feasibility of FEP/H-REMD calculations within a QM/MM framework augmented by the FIRES partitioning scheme in the context of ion hydration. As a first illustrative application of the method, we consider two cations, Na^+ and K^+, and two anions, Cl^- and Br^-. These choices are motivated by the abundance of experimental data on structural and thermodynamic properties of aqueous solutions available. We also examine basis set issues for the QM region as well as the impact of number of solvent molecules treated on QM and MM levels on the computed relative free energies.

The outline of the article is as follows. In the next section (Methodology), we will describe the details of simulations and provide the necessary theoretical background. This section is followed by discussion of the relative free energy estimates from FEP/H-REMD with QM/MM simulations, FIRES QM/MM simulations of solvent reorganization around an ion (Results and Discussion), and comparisons to simulations with Drude polarizable force-field.[19,20,24] In the last section of the article (Conclusion), we will summarize the main results of the work.

II. METHODOLOGY

(i). FEP Calculations Based on a QM/MM Treatment. We extend FEP simulations using previously proposed protocol.[48,49,53] Briefly, the computational scheme employs a standard free energy perturbation protocol by slowly changing the system from one state to another through a number of intermediate alchemical steps. The Hamiltonian controlling this perturbation can be written as

$$H(\lambda, t) = \lambda H_A(t) + (1 - \lambda)H_B(t)$$

where subscripts A and B corresponds to the initial and final states of the system. The corresponding Hamiltonians (H_A and H_B) share all of the objects in the mixed system (QM/MM). The perturbation parameter (λ) is used to evolve one state to another. The parameter λ is changing in a range of values between 0 and 1, with $\lambda = 0$ representing state A and $\lambda = 1$ representing state B of the perturbation path. An excellent review of the method and its applications was provided by Li et al.[42]

Two different QM/MM setups were used in this work. To test the performance of different basis-sets, we considered a water droplet large enough to cover at least two solvation layers around an ion (21 molecules together). The number of QM water molecules in this droplet was varied from 6 to 16. The second QM/MM system consists of 16 QM solvent molecules, 1 QM ion and 234 TIP3P water molecules to approximate bulk solvation. The dispersive correction (C6) was used for most of the QM simulations and for QM/MM runs. The relative free energies of ion hydration show no significant dependence on presence of C6. The differences due to matching interaction energies between QM and MM regions can be as large as several kcal/mol.[54−57] To obtain the correct state distribution between the QM and MM regions, Lennard-Jones parameters corresponding to the interaction energies between QM and MM particles were adjusted with a method previously described.[52]

The molecular dynamics simulations were performed using the leapfrog algorithm with a 2 fs time step. The TIP3P water model was used to model the MM molecules. The temperature was maintained using a Langevin thermostat set to 298.15 K with a friction coefficient of 25 ps^{-1} acting on heavy atoms only. All of the MM water molecules were kept rigid using the

SHAKE algorithm. All FEP calculations based on QM/MM simulations were performed using a modified version of CHARMM c36a4 interfaced with deMon 2.5.7 (modified).[53,58] The "gukini.src" source file, which contained the CHARMM/GAMESS and CHARMM/Q-Chem[49,59] interfaces, was altered to include deMon2k as the external quantum chemistry program. Several different basis sets including 6-31++G**, DZVP-GAA, 6-311++G(2d,2p), def2-TZVPPD, and aug-cc-pVDZ were employed to test the basis set dependence. All-electron basis sets with additional higher-angular momentum basis functions to represent electron polarization and additional diffuse basis functions (two sets for 6-311++G(2d,2p) and def2-TZVPPD) were used to study the ions. The grid tolerance was set to 10^{-5} for the exchange-correlation integration and a tolerance of 10^{-5} (for Cl^-/Br^-) and 10^{-4} (for K^+/Na^+) Hartrees was used in the SCF iterations. These parameters were found to produce a reasonable accuracy/performance ratio in a series of MD test simulations.[53,58] The exchange-correlation functional used for simulations of the ion solvation was PBE98-PBE, as implemented in deMon2k.[21,22] The choice of PBE98-PBE functional for QM/MM simulations was based on previous testing of DFT performance for studies ion−water cluster thermodynamics.[58] The systems for the QM/MM DFT calculations were first equilibrated with classical MD simulation (2 ns per window) and then re-equilibrated for 1 ps per window, prior to the production run of the FEP λ−windows. Forward and backward simulations were performed for all of the systems studied with 11 λ windows connecting the initial and final states of the system.

(ii). FEP/H-REMD Calculations with QM/MM Simulations. The completeness of the sampling and apparent dependence on the starting configuration are well-known hurdles in short-time scale simulations that are typically accessible by QM dynamics. To circumvent these limitations, we employ H-REMD along with the FEP scheme to obtain free energy differences between pairs of ions. In FEP/H-REMD, each window of the replica represents an alchemical state that corresponds to a specific λ value from the dual topology Hamiltonian used for the perturbation reaction. The H-REMD algorithm periodically exchanges coordinates between replicas. The probability of exchange is defined as

$$P(q_i \rightarrow q_j) = \min\{1, e^{-[U_i(q_j)+U_j(q_i)-U_i(q_i)-U_j(q_j)]}\}$$

where U is the potential energy and subscripts i and j represent the replica number. The window spacing was chosen to produce an acceptance ratio of ∼0.3 in accordance with previous work on FEP/H-REMD[60] method.

(iii). FIRES Partition: Flexible Boundaries between QM and MM Regions. The FIRES method was used to separate the system into QM and MM regions.[52,61] The FIRES formulation is similar in spirit to the mixed explicit-implicit system representation known as Spherical Solvent Boundary Potential (SSBP).[62] In QM/MM simulations with FIRES, a set of n solvent molecules nearest to a solute is treated at the QM level, while the rest of the system is represented with a chosen MM force field. The n was varied in our simulations to study the dependence of the relative solvation free energies on the number of coordinating ligands, and the confinement radius was estimated based on the bulk density of water. A separation of the configurational integral with identical solvent molecule is formally exact and is independent of the choice of potential function.[52] The boundaries between QM and MM regions of the system are flexible, and a restraining force is imposed to prevent MM molecules from penetrating the sphere defined by radius R_{in}. The constraint also ensures that the QM solvent molecules remain nearest to the ion. A force constant of 500 kcal $Å^{-2}$ was effective at maintaining this condition.[52]

$$R_{in} = \max(|r_1|, ..., |r_N|);\ E_{FIRES} = \sum_{j=n+1}^{N} \frac{k_{FIRES}}{2}(r_j - R_{in})^2$$

This procedure does not introduce any significant artifacts into the MD simulation results,[52] but its usefulness for QM/MM FEP is yet to be established. An example of the solvation shell separation into QM and MM regions is illustrated in Figure 1. The first solvation shell is expected to dynamically adjust to an ion type during perturbation and FIRES shall be able to account for it.

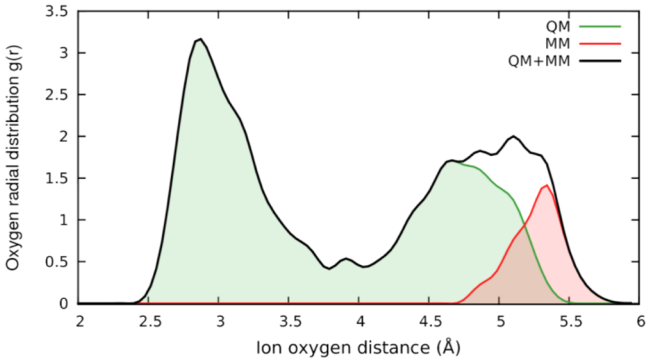

Figure 1. QM/MM decomposition of the system. The oxygen-ion radial distribution function and its quantum and classical components for solvated K^+. The droplet is composed of 16 QM and 234 MM waters. The flexible boundaries were implemented by the FIRES protocol.

III. RESULTS AND DISCUSSION

The results for the free energy perturbation for a pair of cations and anions are shown in Tables 1 and 2 for various compositions of the QM solvation shell and combinations of basis sets in comparison to experimental data.[63−66] One general trend is that basis sets that account for both polarization and dispersion terms tend to perform better than less-intensive computational choices. Nevertheless, a majority of the results presented in these two tables are in agreement with both experimental and previous free energy simulations performed with both classical and polarizable force fields.[16,19,20,24,67,68] The results from the FEP calculations are encouraging and show that developed scheme can be readily used to blinded studies of ion solvation providing sufficient quality of functional/basis-set combinations.

(i). Estimation of Relative Free Energies of Ion Hydration (ΔΔ*G*) from QM/MM Simulations. *Basis Set Dependence of ΔΔG.* Our previous studies showed that $\Delta\Delta G_{K+/Na+}$ in water droplets starts to approach bulk-like values for $n \geq 6$.[58] Accordingly, we chose to study QM droplets with n = 6 and 8 as a function of the basis set. The resulting free energies are very sensitive to the basis set choice. This result can be illustrated by the K^+/Na^+ relative free energy differences in the droplet containing 8 QM water molecules (Table 1). The confining potential for QM or QM/MM clusters, defined as a function of the distance R between the ion and the oxygen

dx.doi.org/10.1021/ct400296w | J. Chem. Theory Comput. 2013, 9, 4165−4175

Table 1. FEP Results for Potassium to Sodium Perturbation for Various Basis Sets and System Compositions[a]

system	functional/basis-set	sampling	$\Delta\Delta G$
6 QM waters	PBE98-PBE/6-311++G(2d,2p)	50 ps	−17.2 ± 0.4
8 QM	PBE98-PBE/6-31++G**	70 ps	−18.7 ± 0.4
8 QM	PBE98-PBE/6-311++G(2d,2p)	80 ps	−17.3 ± 0.2
	QM/MM System 1		
8 QM + 13 MM (FIRES)	PBE98-PBE/6-311++G(2d,2p)	90 ps	−16.1 ± 0.2
8 QM + 13 MM (FIRES+H-REMD)	PBE98-PBE/6-311++G(2d,2p)	90 ps	−15.8 ± 0.3
12 QM + 9 MM (FIRES+ H-REMD)	PBE98-PBE/6-311++G(2d,2p)	200 ps	−17.4 ± 0.2
16 QM + 5 MM (FIRES+ H-REMD)	PBE98-PBE/6-311++G(2d,2p)	70 ps	−18.1 ± 0.1
16 QM + 5 MM (FIRES+ H-REMD)	PBE98-PBE/DZVP-GGA	70 ps	−18.7 ± 0.1
	QM/MM System 2		
16 QM + 234 MM (FIRES + H-REMD)	PBE98-PBE/6-31++G**(water)/ 6-311++G(2d,2p)(ions)	∼110 ps	−21.5 ± 0.2
	Available Experimental Data		
extra thermodynamic hypothesis	Schmid et al.[65]		−17.4
aqueous cluster measurements	Tissandier et al.[63]		−17.2
aqueous cluster measurements	Klotts[66]		−17.6
electrochemical measurements	Gomer et al.[64]		−17.6

[a]Free energy difference is presented in kcal/mol. Standard deviations for WHAM calculations were estimated using block averaging over 3 blocks.

Table 2. FEP Results for Chloride to Bromide Perturbation for Various Basis Sets and System Compositions

system	functional/basis-set	sampling	$\Delta\Delta G$
8 QM	PBE98-PBE/def-TZVPPD	88 ps	5.1 ± 0.3
16 QM	PBE98-PBE/def2-TZVPPD(ions)/ 6-31++G**(water)	88 ps	5.7 ± 0.2
	QM/MM System 1		
8 QM + 13 MM (FIRES+ H-REMD)	PBE98-PBE/def2-TZVPPD	90 ps	4.6 ± 0.2
16 QM + 5 MM (FIRES+ H-REMD)	PBE98-PBE/def2-TZVPPD	60 ps	5.2 ± 0.2
	QM/MM System 2		
16 QM + 234 MM (FIRES/H-REMD)	PBE98-PBE/def2-TZVPPD(ions)/6-31++G**(water)	110 ps	6.5 ± 0.2
	Available Experimental Data		
extra thermodynamic hypothesis	Schmid et al.[65]		6.5
aqueous cluster measurements	Tissandier et al.[63]		6.4
aqueous cluster measurements	Klots[66]		3.3
electrochemical measurements	Gomer et al.[64]		5.3

ligands, is equal to $K(R - 4.0)^2$ when $R > 4.0$ Å, and zero otherwise. The force constant, K, is equal to 50 kcal/mol/Å^2 and based on series of tests the precise value of K has no significant impact on the results. The double-ζ 6-31++G** basis set yields $\Delta\Delta G_{K+/Na+}$= −18.7 kcal/mol, which slightly overestimates the experimental free energy difference. The introduction of additional diffuse and polarization functions into the basis set (triple-ζ 6-311++G(2d,2p)) led to a decrease in the computed relative free energies($\Delta\Delta G$ = −17.3 kcal/mol), which compares well to the experimental data. Relatively small basis sets, such as 6-31++G** and DZVP-GAA, led to the overestimation of $\Delta\Delta G$ (i.e., −18.1 and −18.7 kcal/mol, respectively). The 6-311++G(2d,2p) basis set results in $\Delta\Delta G$ = −17.9 kcal/mol. This trend, which was observed for small QM systems, is also observed for a larger QM/MM system containing 16 QM waters simulated using the FIRES methodology to separate the QM and MM shells and replica-exchange for enhancing the sampling (Table 1). Cl^- to Br^- perturbation displays even stronger dependence on the quality of the basis set used to represent the system. FEP simulations using the aug-cc-pVDZ double-ζ basis set with a single set of diffuse and polarization basis functions results in $\Delta\Delta G$ = 4.5−5.5 kcal/mol. The most extensive basis set (i.e., def2-TZVPPD, a triple-ζ basis set with two sets of polarization and one set of diffuse basis functions) results in $\Delta\Delta G_{Cl^-/Br^-}$ = 5.2 to 5.7 kcal/mol. Interestingly, the use of a smaller basis for the solvent molecules (Table 2) along with the def2-TZVPPD basis set for the ion offers a reasonable trade-off for the computed free energy difference. In addition, the inclusion of the replica-exchanges (RE) sampling does not significantly affect the results of the FEP calculations. It should be noted that most of the systems studied in this work are small aqueous clusters that can be sampled in relatively short simulations, which are computationally accessible to QM/MM methods. For larger protein-sized QM/MM systems, the inclusion of RE into the algorithm is expected to considerably enhance the sampling.

ΔΔG Dependence on the Composition of the Simulated System. The composition of the droplet (e.g., the ratio of QM and MM waters) plays an important role in the determination of the solvation thermodynamics. For example, FEP simulations for the system with 8 QM and 13 MM waters results in a relative free energy differences ($\Delta\Delta G_{K+/Na+}$) of approximately 16 kcal/mol, which differs from the experimental value for the solvation in the bulk. Ion solvation by the droplet composed of 12 QM and 9 MM water molecules results in $\Delta\Delta G_{K+/Na+}$= −17.4 kcal/mol, while the system with 16 QM and 5 MM water molecules results in $\Delta\Delta G_{K^+/Na^+}$= −17.9 kcal/mol. These results suggest that the sub-kcal accuracy of FEP methods is sensitive to the treatment of ion interactions with water molecules in the second or even third solvation shell. To test the performance of the developed methods for a bulk-like system, we ran QM/MM simulations for a system composed of 1 ion and 250 solvent molecules where 16 waters were treated quantum mechanically. The calculation using the current CHARMM implementation is prohibitively slow for large basis sets. Therefore, we chose to use PBE-PBE/6-31++G** to represent solvent and 6-311++G(2d,2p) basis set to represent ions. An increase in the size of the solvation shell and change in water representation (as compared to the droplet with 21 molecules) led to a relative solvation energy of ∼-21.5 kcal/mol for K^+/Na^+ perturbation.

The relative solvation free energy is 6.5 kcal/mol for Cl^-/Br^- perturbation in QM/MM system. The anions were represented by def2-TZVPPD basis set and water was described with 6-31++G** basis set. The same combination of basis sets and functional for a water cluster made of 16 QM water molecules only resulted in relative free energy of 5.7 for Cl^-/Br^- perturbation, which is within uncertainty of the method.

(ii). Analysis of Structural Properties. *Solvent Reorganization along the Reaction Coordinate with FIRES.* The evolution of ion−oxygen and oxygen−oxygen distribution functions along the perturbation coordinate is shown in Figures 2 and 3. The evolution of these RDFs display smooth changes

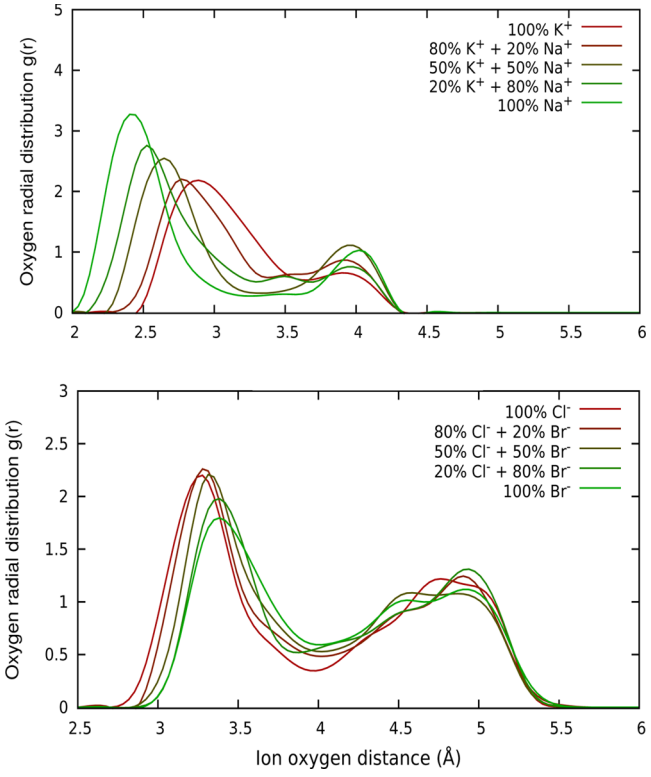

Figure 2. Top: Evolution of the oxygen-ion radial distribution function for K^+/Na^+ perturbation. The droplet is composed of 8 QM waters. Bottom: Evolution of the oxygen-ion radial distribution function for Cl^-/Br^- perturbation. The droplet is composed of 16 QM waters.

in the position of the first peak (ion−oxygen RDF) with well-defined separation between the first and second solvation shells for a smaller ion. The oxygen−oxygen RDFs (Figure3) display a sharp first peak at the position $R \sim 2.8$ Å in good agreement with the results of Bankura et al.[69] While the oxygen−oxygen RDFs for the transition between Cl^- and Br^- are virtually identical across the entire perturbation path, the intermediates describing the transition from K^+ to Na^+ display variation in structuring around 3.5−4.5 Å along the path and for the end-points. This distance corresponds to a tetrahedral structure of water and reflects the influence of a solvated ion on the first and second solvation shell. The computed $\Delta\Delta G$ values display excellent agreement with experimental values, suggesting that FIRES allows for dynamical adaptation of the first solvation shell along the reaction path. To further validate performance of the present FEP/H-REMD calculations based on QM/MM simulations augmented by the FIRES separation scheme, we investigated structural properties of studied systems.

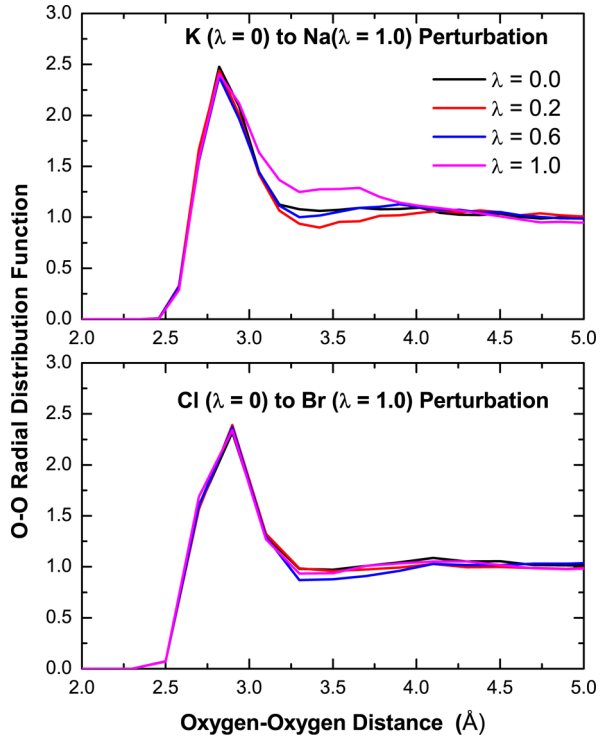

Figure 3. Oxygen−oxygen RDF for QM waters along the λ-coordinate.

Structural Aspects of Na^+ Solvation. The first hydration shell of Na^+ is considered to be well-defined with 5 to 6 coordinating water molecules. The ion−water distribution function is sharp and narrow, and a relatively narrow first peak that is well separated from the second solvation shell was obtained. The evolution of the radial distribution function for $Na^+ \rightarrow K^+$ perturbation is shown in Figure 2 for the system with 8 QM water molecules in the droplet. The maximum RDF(r_{max}) for the hydrated Na^+ is located ~2.4 Å. The neutron diffraction data provides an average nearest-neighbor Na−O distance of 2.40 ± 0.05 Å,[70] and recent LAXS data led to an average Na−O distance of 2.43 ± 0.02 Å.[71] The width of the peak is in good agreement between MD simulations using a polarizable force field reported earlier and experimental methods showing a deep minimum between 3.0 Å and 3.5 Å. Because of the restriction in the shell-size, it is not feasible to assess the packing in the second shell. The height of the first peak shows considerable variability. Our QM/MM simulations show the height of the first peak at ~3.4, while recent DFT, MP2 QM/MM, and Drude MD simulations[52] predict peaks at 5.3, 6.0, and 6.8, respectively. The inclusion of the complete second and third solvation layers into the simulations led to an improvement in the RDF description compared to the experimental data. The position of the first peak in the RDF is unchanged, while the peak's height increased to 5.3, which is in good agreement with the results from previous studies (Figure 3). Similar trends are observed in $n(r)$, shown in Figure 3. At $r = 3.2$ Å, $n(r)$ for the MP2 and Drude models are very close to each other (5.6 and 5.8, respectively).[52] Our QM/MM simulations with 16 QM and 234 MM water molecules predict a lower coordination number with $n = 5.3-5.4$ (Figures 4 and 5). In addition, our results show an extended flat region suggesting a separation between the first and second solvation shells. The distribution of the coordination states for the

dx.doi.org/10.1021/ct400296w | J. Chem. Theory Comput. 2013, 9, 4165−4175

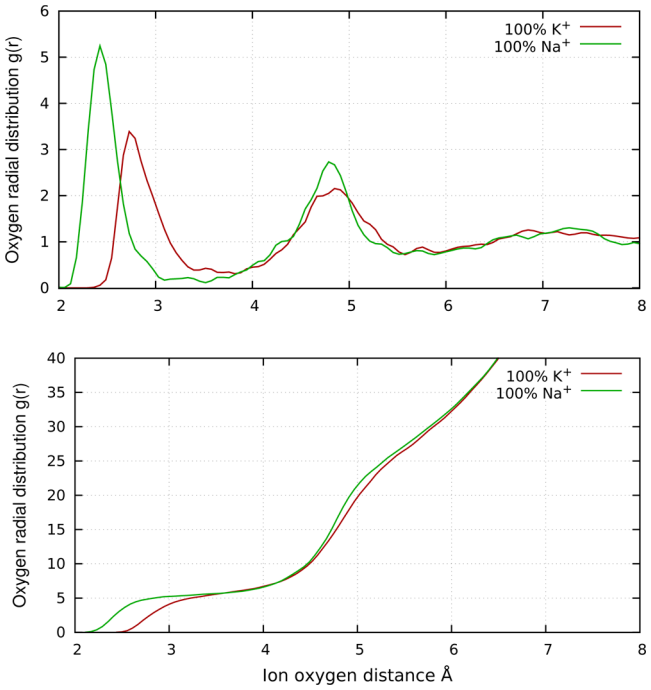

Figure 4. Ion−oxygen RDFs for solvated Na^+ and K^+ for QM/MM FEP simulations (solvent composition: QM = 16/MM = 234).

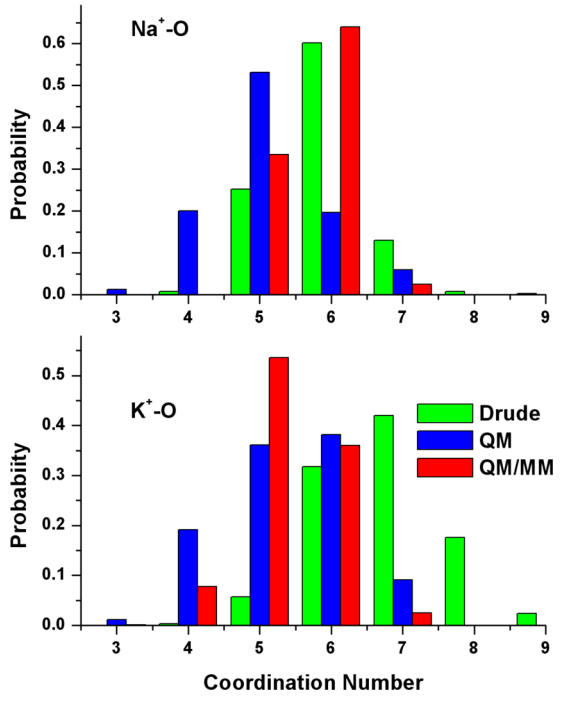

Figure 5. Distribution of hydration states for Na^+ and K^+ for QM/MM FEP simulations (solvent composition: QM = 16/MM = 234).

hydrated Na^+ ion is shown in Figure 5 for the QM/MM simulations performed for clusters composed of 8 QM waters, 16 QM/234 MM waters, and bulk simulations with the polarizable Drude model for the ion and solvent molecules. An inclusion of the complete second and third solvation shells via MM molecules (QM system 2) combined with a relatively small basis set to describe the water molecules led to an overestimation of the relative free energies of solvation where $\Delta\Delta G = -21.5$ kcal/mol. The DFT-based computations suggest a shift in the most probable coordination from $n = 6$ (Drude) to $n = 5.3$. The DFT CPMD studies published to date also led to a penta-coordinated Na^+ in solution with the use of PBE functional ($n = 4.9$) even though PBE-D displays an average coordination of $n = 5.8$.[69]

Structural Aspects of K^+ Solvation. Potassium is thought to be the first alkali cation with a relatively diffuse coordination sphere and a broad distribution of the possible coordination states. In good agreement with this general image of the hydrated ion, QM/MM simulations of K^+ indicates a broad first peak in the ion−oxygen RDF with the first peak located at ∼2.82 Å, which is in excellent agreement with the previously reported simulations using additive, polarizable, and QM representations of the Hamiltonian.[19,20,24,52] This result is also in agreement with the average nearest-neighbor K−O distance of 2.73 ± 0.05 Å determined by EXAFS[72] and the K−O distance of 2.81 ± 0.01 Å determined by LAXS.[71] However, this value is considerably larger than the r_{max} = 2.65 Å determined from neutron diffraction.[73] Similar to the results from the Na^+ simulation, the maximum height of the first peak in the RDF produced by our calculations is the lowest with a $g(r_{max})$ of ∼2.2 compared to other methods reporting a value between 3.5 and 4.5. Inclusion of the complete solvation layers led to a significant increase in the peak's height to ∼3.5, which suggested the important role of packing of the second solvation shell. The running integration number, $n(r)$, is continuously increasing and does not plateau as in the Na^+ case. This process is illustrated in Figure 2 where the change in the shape of $n(r)$ is especially noticeable upon perturbation of the ion. This finding is consistent a broad and diffuse first coordination shell of K^+ in solution. The distribution of the coordination numbers is shown in Figure 3. The most probable coordination number for K^+ in the water droplet and in a bulk-like QM/MM system is 6.1 and 6.4, respectively. The distribution of states (Figure 5) display a significant fraction of penta- and hexa-coordinated hydration states. The width of the distribution is significantly broader that that for Na^+ ranging from $n = 4$ to $n = 8$. A similar distribution for the K^+ hydration sphere from the MD simulations with a polarizable force field shows a shift in the most probable coordination state to $n = 7$ with $n = 6$ almost as likely (Figure 4). The width of the distribution is similar to that from QM but it is shifted toward larger coordination numbers.

Angular Distributions of Water Molecules around Cations. The structural aspects of the solvent distribution around an ion can also be characterized by studying the tilt and angular distribution in the first solvation shell. It should be noted that the Drude model displays a very reasonable agreement with the results from the QM/MM simulations. The tilt distribution (ion−oxygen−hydrogen) is shown in Figure 6 for Na^+ and K^+. For Na^+, the QM/MM simulations show a smooth decline in the region between −1 and −0.25 for Na^+ and a pronounced flat region between −1 and −0.75 for K^+. The angular distribution characterizing the angles formed between the ion and two water oxygens is shown in Figure 7. The ADF for the QM, QM/MM and Drude simulations displays a well-pronounced peak at $\cos\theta = 0.0$ ($\theta = 90°$) and a second peak at $\cos\theta \sim -1.0$ ($\theta = 180°$), which is in agreement with previous studies. The ADF distribution is slightly different for K^+ where both peaks are less pronounced and the first peak is shifted toward $\cos\theta \sim 0.2$. The corresponding peak for the Drude simulations is also shifted to $\cos\theta = 0.1$. It is important to note that the peak at $\cos\theta = -1.0$ decreased in the Drude, QM and QM/MM simulations. Accounting for the outer MM

dx.doi.org/10.1021/ct400296w | J. Chem. Theory Comput. 2013, 9, 4165−4175

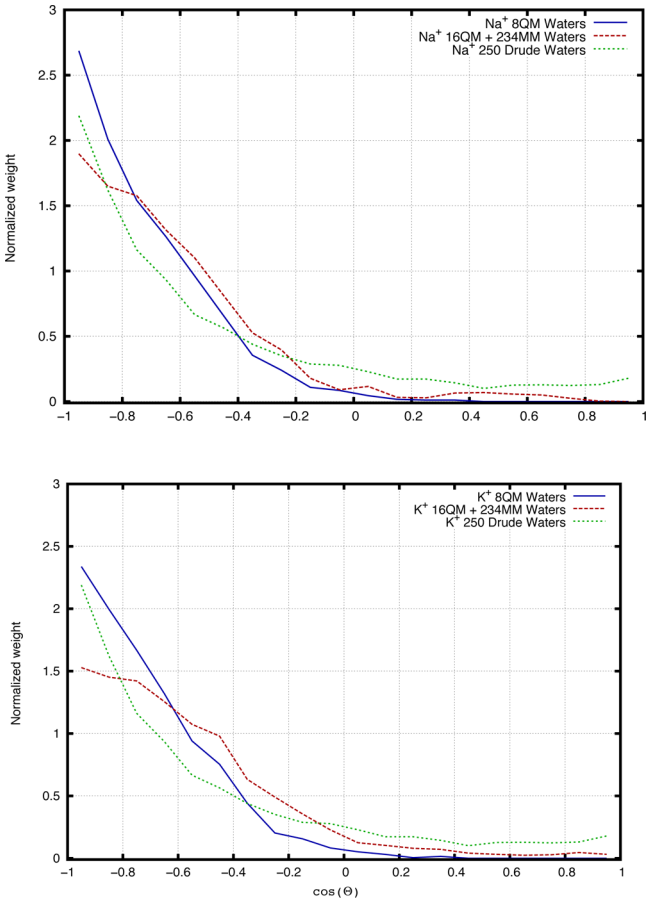

Figure 6. Ion−oxygen−hydrogen angular distribution function (ADF) for Na^+ and K^+ simulations with polarizable force field (Drude), QM, and QM/MM systems.

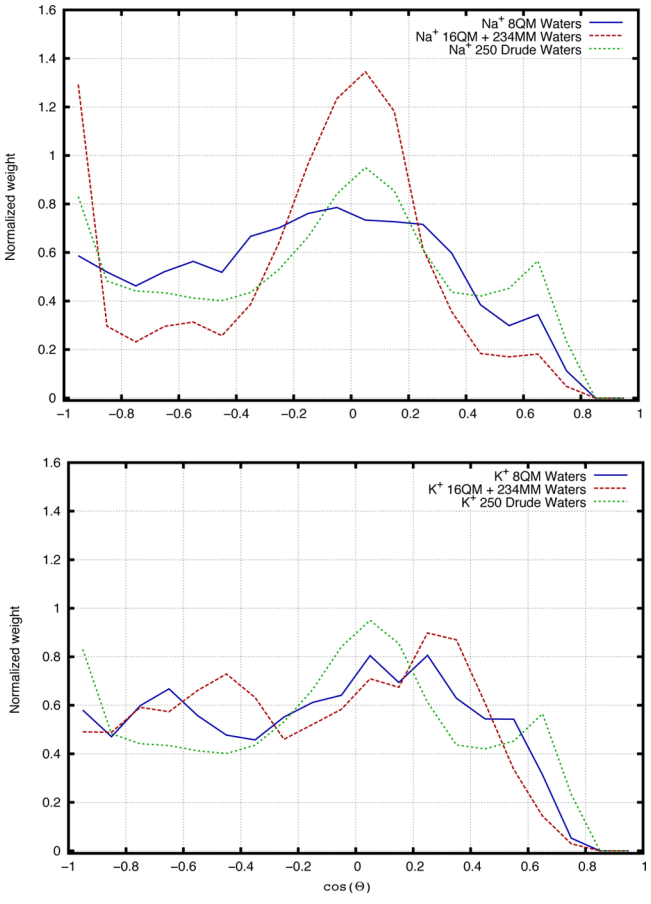

Figure 7. Oxygen−ion−oxygen ADF for Na^+ and K^+ simulations with polarizable force field (Drude), QM, and QM/MM systems (solvent composition: QM = 16/MM = 234).

layer in the QM/MM simulation led to a well-defined angular distribution. However, the use of a cluster model tended to produce a flatter distribution while retaining most of its characteristic features.

Structural Aspects of Cl^- Solvation. The Cl^- hydration has been extensively studied both experimentally and theoretically. The pronounced first peak and better separation between the first and second solvation shell suggest (Figure 8) that the first coordination sphere is more structured that that for another anion studied in this paper. The position of the first peak in RDF(r_{max}) is 3.21 Å, which is in excellent agreement with the available experimental data (3.1 to 3.3)[1] and DFT and *ab initio* MD simulations.[42,74] The average coordination number for solvated Cl^- is estimated to be n = 5.5 from simulations with QM representation and n = 5.9 from the QM/MM simulations, which is similar to experimentally determined value of n = 6.0.[75] The distribution of the coordination states suggests a nearly equal presence of penta- and hexa-coordinated ion−water complexes, while all of the other coordination states do not significantly contribute. The coordination numbers from the MD simulations using polarizable force fields suggest higher coordination numbers with two dominant coordination states at n = 7 and 8.

Structural Aspects of Br^- Solvation. The structural aspects of Br^- hydration were evaluated only recently by a combination of EXAFS as well as classical and quantum MD simulations,[35] which offers us a chance to compare the performance of the water cluster approximation for large polarizable ion hydration.

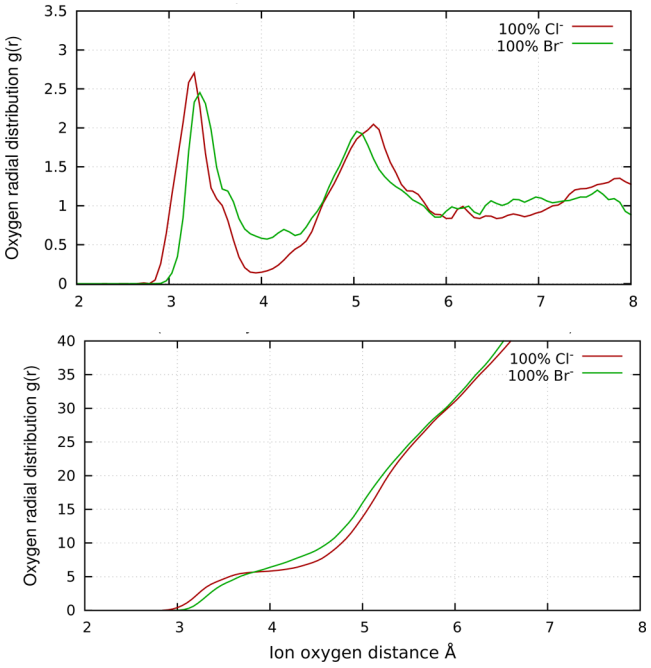

Figure 8. Ion−oxygen RDFs for solvated Cl^- and Br^- for QM/MM FEP simulations (solvent composition: QM = 16/MM = 234).

The position of the first peak in the RDF(r_{max}) from both the QM and QM/MM simulations is at 3.4 Å, which is in excellent

dx.doi.org/10.1021/ct400296w | J. Chem. Theory Comput. 2013, 9, 4165−4175

agreement with EXAFS (3.35 to 3.4 Å)[76,77] and AXS (3.35 Å) data.[78] CPMD simulations show that the position of the first peak is shifted to slightly shorter distances with a RDF(r_{max}) between 3.2 to 3.3 Å.[35] The data for the ion−water RDFs shown in Figures 8 and 9 display significant probabilities for

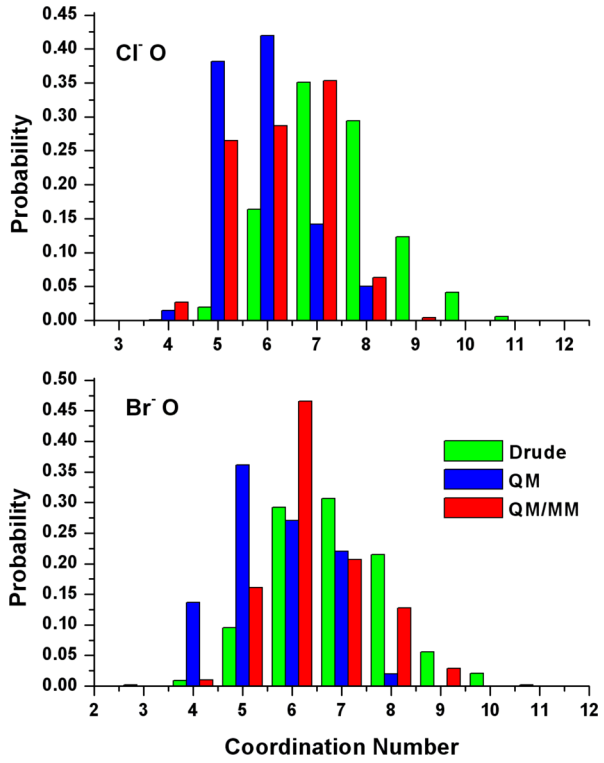

Figure 9. Distribution of hydration states for Cl^- and Br^- for QM/MM FEP simulations.

finding the water molecule in the region between the first and second solvation shell, which suggests a high exchange probability and a diffuse solvation shell surrounding the bromide ion. Previously reported classical MD simulations show primarily 7- and 8-fold coordination complexes of hydrated Br^-, which is in agreement with the results from simulations using the polarizable force field (Drude). The same CPMD simulations led to a coordination of 5- or 6-fold for the ion.[79] The available experimental data suggest the most probable coordination number to be approximately 7.[76,77] The distribution of the coordinated states for both studied anions is shown in Figure 9. The QM FEP results reported in Figure 9 show a broad distribution with n = 5, 6, and 7 representing a large fraction of the total population of states. The average coordination number is 5.6 and 6.6 for QM and QM/MM simulations, respectively. This result is in agreement with recent report from D'Angelo[35] et al. (6.5) and contrasts with earlier studies by Raugei and Klein[79] (5.1).

Angular Distributions for Anions. To provide additional insight into the organization of the solvation shell around anions, we computed the angular distribution functions. The tilt distribution (ion−oxygen−hydrogen) is shown in Figure 10 for Cl^- and Br^-. For both ions, the results from the Drude, QM, and QM/MM simulations show a well-pronounced peak positioned at cos θ = 0.6 (53.1°) for Cl^- and cos θ = 0.62 (51.7°) for Br^-. The peak ranges in width from 0.2 to 0.8. These results are in agreement with the data obtained from CPMD simulations reported by D'Angelo et al.[35] with a

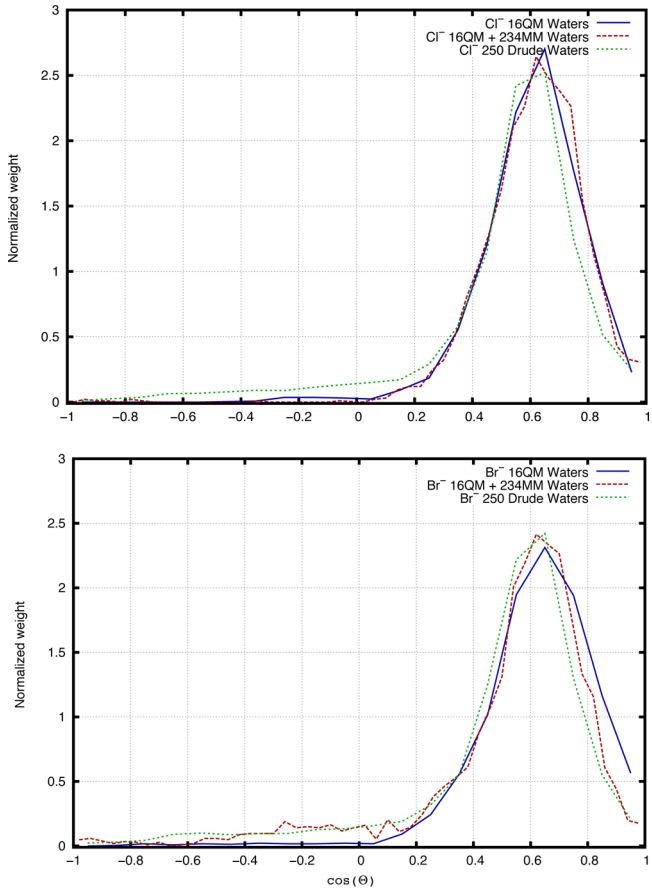

Figure 10. Ion−oxygen−hydrogen angular distribution function (ADF) for Cl^- and Br^- simulations with polarizable force field (Drude), QM, and QM/MM systems.

distribution maxima at θ = 55.3°. The Drude simulations were able to return the proper angular distributions without any adjustments. In addition, the height and width of the distribution is in good agreement with the QM data. These distributions indicate a nearly linear water hydrogen bond to the ion (anion−H−O).[79] The broadness of the first peak indicates that the first solvation shell of both anions exhibit rather large flexibility. The angular distribution characterizing the angles formed between an anion and two water oxygens is shown in Figure 11. Unlike the tilt distribution, it does not exhibit a well-pronounced peaks, which is in agreement with data of D'Angelo[35] and in disagreement with the results of Raugei and Klein.[79] For Cl^-, a broad peak was found at cos θ = 0.1 to 0.2 (QM and QM/MM) and cos θ = 0.35 (Drude). The ADF for Br^- contains two broad peaks (QM/MM and Drude) at approximately cos θ = −0.75 and cos θ = 0.4. It should be noted that QM/MM displays a greater probability of the peak at cos θ = −0.75 (138.6°), while the Drude simulations favor the cos θ = 0.4 (66.4°) orientation.

Comparison of QM/MM and Polarizable Force-Fields. In that the present study, simulations employing Drude models for water and monovalent ions provide good agreement with QM and QM/MM simulations. Nevertheless, explicit treatment may be necessary for studies of ion solvation. For example, Riahi et al[61] recently compared performance of MD simulations with classical, polarizable and QM/MM Hamiltonians by studying aqueous solvation of Zn^{2+} and Mg^{2+} with MD and Thermodynamic Integration (TI) simulations. While all of the

dx.doi.org/10.1021/ct400296w | J. Chem. Theory Comput. 2013, 9, 4165−4175

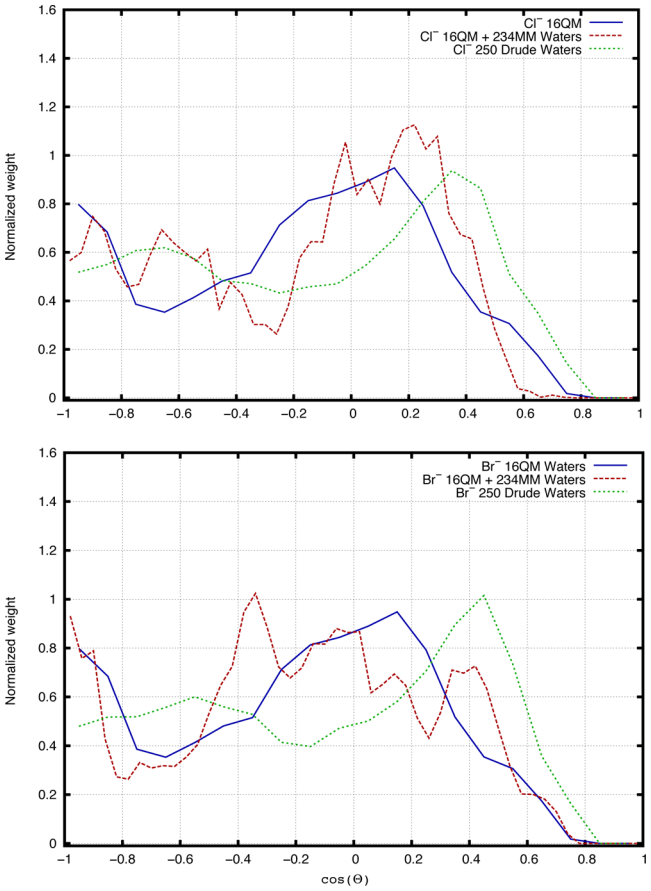

Figure 11. Oxygen−ion−oxygen ADF for Cl^- and Br^- simulations with polarizable force field (Drude), QM, and QM/MM systems.

methods were capable of reproducing structural information such as distribution function, simulations with classical force fields failed to reproduce free energy difference between two ionic species in case of divalent cations. An important conclusion is that the correct representation of the structural properties (ion−water radial distribution functions) by a force field does not imply an accurate description of the resulting thermodynamics and visa versa.[61] Therefore, matching structural properties or the free energy of solvation alone is not a unique benchmarks of the force field performance.[3] The methods developed in this paper may offer direct route for obtaining accurate thermodynamic AND structural information at the same time thus providing information for future force-field development for simulations of ion solvation.

IV. CONCLUSIONS

We have performed FEP/H-REMD calculations based on QM/MM simulations using the FIRES partition scheme to study the solvation of Na^+/K^+ and Cl^-/Br^- in water. The methodology was implemented as an extension of the CHARMM-DeMon2k interface.[58] We evaluated performance of different basis-sets for the FEP calculations of thermodynamics of monovalent ions hydration. Enhanced sampling with H-REMD resulted in modest difference in computed $\Delta\Delta G$ compared to standard FEP studies of ion pairs. It was also found that correct description of anion hydration requires larger number of water molecules to be treated quantum-mechanically. Standard FEP for pair of anions combined with H-REMD led to significant improvement in computed relative free energy of hydration. To prevent rapid exchanges of solvent molecules between QM and MM parts of the system, we extended for the first time the FIRES protocol to enable FEP simulations. DFT-based QM and QM/MM simulations tend to modestly overestimate the relative free energy of solvation of the K^+/Na^+ and Cl^-/Br^- pairs and underestimate the size of the ion's coordination sphere compared to simulations with the Drude polarizable model. However, the main conclusion is that overall correlation between simulations with polarizable force field and FEP/H-REMD with QM/MM is quite impressive for monovalent ion hydration. Analysis of RDFs evolution along the permeation path suggests that FIRES allows for adequate relaxation and restructuring of the solvation shell around an ion during FEP run. Our results are in agreement with previously published CPMD, thermodynamical data available, and diffraction studies. Therefore, it can be concluded that FEP calculations based on QM/MM combined with H-REMD can be used to directly investigate ion solvation to provide reliable estimate for relative thermodynamics between different ions.

AUTHOR INFORMATION

Corresponding Author

*Phone: 1-773-834-3557 (B.R.) or 1-403-210-7971 (S.N.). E-mail: snoskov@ucalgary.ca or roux@uchicago.edu.

Present Address

[§]Health Innovations Research Institute, RMIT University, Melbourne, Victoria 3001, Australia

Notes

The authors declare no competing financial interest.

ACKNOWLEDGMENTS

This work has been supported by the Natural Sciences and Engineering Research Council (NSERC) Discovery grant program (RGPIN 340946-07), the Natural Science Foundations (MCB-0920261), and a Resource Allocation Award from WestGrid, Canada. S.N. is an Alberta Innovates Technology Futures (AITF) New Faculty, and B.L. was a recipient of AITF graduate scholarship. The discussions with Dennis R. Salahub are greatly acknowledged.

ABBREVIATIONS

QM, Quantum Mechanics; MM, Molecular Mechanics; MD, Molecular Dynamics; H-REMD, Hamiltonian Replica-Exchange MD; FEP, Free Energy Perturbations; FIRES, Flexible Inner Region Ensemble Separator

REFERENCES

(1) Ohtaki, H.; Radnai, T. Structure and Dynamics of Hydrated Ions. *Chem. Rev.* **1993**, *93*, 1157−1204.

(2) Marcus, Y. A Simple Empirical-Model Describing the Thermodynamics of Hydration of Ions of Widely Varying Charges, Sizes, and Shapes. *Biophys. Chem.* **1994**, *51*, 111−127.

(3) Roux, B.; Bernèche, S.; Egwolf, B.; Lev, B.; Noskov, S. Y.; Rowley, C. N.; Yu, H. Ion Selectivity in Channels and Transporters. *J. Gen. Physiol.* **2011**, *137*, 415−426.

(4) Mishra, A. K.; Ramaprabhu, S. Functionalized graphene sheets for arsenic removal and desalination of sea water. *Desalination* **2011**, *282*, 39−45.

(5) Sint, K.; Wang, B.; Kral, P. Selective Ion Passage through Functionalized Graphene Nanopores. *J. Am. Chem. Soc.* **2008**, *130*, 16448−16449.

(6) Hou, X.; Guo, Y.; Jiang, L. Biomimetic smart nanopores and nanochannels. *Chem. Soc. Rev.* **2011**, *40*, 2385−2401.

(7) Roux, B. Ion Binding Sites and Their Representations by Reduced Models. *J. Phys. Chem. B* **2012**, *116*, 6966−6979.
(8) Åqvist, J. Ion Water Interaction Potential Derived from Free Energy Perturbation Simulations. *J. Phys. Chem.* **1990**, *94*, 8021−8024.
(9) Cornell, W. D.; Cieplak, P.; Bayly, C. I.; Gould, I. R.; K. M., M., Jr.; Ferguson, D. M.; Spellmeyer, D. C.; Fox, T.; Caldwell, J. W.; Kollman, P. A. A Second Generation Force Field for the Simulation of Proteins and Nucleic Acids. *J. Am. Chem. Soc.* **1995**, *117*, 5179−5197.
(10) MacKerell, A. D.; Brooks, B.; C. L., B., III; Nilsson, L.; Won, Y.; Roux, B.; Karplus, M. In *The Encyclopedia of Computational Chemistry*; John Wiley & Sons: Chichester, 1998.
(11) Jensen, M. O.; Borhani, D. W.; Lindorff-Larsen, K.; Maragakis, P.; Jogini, V.; Eastwood, M. P.; Dror, R. O.; Shaw, D. E. Principles of Conduction and Hydrophobic Gating in K+ Channels. *Proc. Natl. Acad. Sci. U.S.A.* **2010**, *107*, 5833−8.
(12) Bostick, D. L.; Brooks, C. L. Selective Complexation of K+ and Na+ in Simple Polarizable Ion-Ligating Systems. *J. Am. Chem. Soc.* **2010**, *132*, 13185−13187.
(13) Yu, H. B.; Ratheal, I. M.; Artigas, P.; Roux, B. Protonation of Key Acidic Residues Is Critical for the K+-Selectivity of the Na/K Pump. *Nat. Struct. Mol. Biol.* **2011**, *18*, 1159−1163.
(14) Yu, H. B.; Noskov, S. Y.; Roux, B. Two Mechanisms of Ion Selectivity in Protein Binding Sites. *Proc. Natl. Acad. Sci. U.S.A.* **2010**, *107*, 20329−20334.
(15) Lev, B.; Noskov, S. Y. Role of the Protein Matrix Rigidity and Local Polarization Effects in the Monovalent Cation Selectivity of Crystallographic Sites in the Na-Coupled Aspartate Transporter. *Phys. Chem. Chem. Phys.* **2013**, *15*, 2397−2404.
(16) Grossfield, A.; Ren, P.; Ponder, J. W. Ion Solvation Thermodynamics from Simulation with a Polarizable Force Field. *J. Am. Chem. Soc.* **2003**, *125*, 15671−15682.
(17) Patel, S.; Mackerell, A. D., Jr.; Brooks, C. L., 3rd CHARMM Fluctuating Charge Force Field for Proteins: II Protein/Solvent Properties from Molecular Dynamics Simulations Using a Nonadditive Electrostatic Model. *J. Comput. Chem.* **2004**, *25*, 1504−14.
(18) Lamoureux, G.; Harder, E.; Vorobyov, I. V.; Roux, B.; MacKerell, A. D. A Polarizable Model of Water for Molecular Dynamics Simulations of Biomolecules. *Chem. Phys. Lett.* **2006**, *418*, 245−249.
(19) Whitfield, T. W.; Varma, S.; Harder, E.; Lamoureux, G.; Rempe, S. B.; Roux, B. Theoretical Study of Aqueous Solvation of K+ Comparing Ab Initio, Polarizable, and Fixed-Charge Models. *J. Chem. Theor. Comp.* **2007**, *3*, 2068−2082.
(20) Yu, H. B.; Whitfield, T. W.; Harder, E.; Lamoureux, G.; Vorobyov, I.; Anisimov, V. M.; MacKerell, A. D.; Roux, B. Simulating Monovalent and Divalent Ions in Aqueous Solution Using a Drude Polarizable Force Field. *J. Chem. Theor. Comp.* **2010**, *6*, 774−786.
(21) Noskov, S. Y.; Lamoureux, G.; Roux, B. Molecular Dynamics Study of Hydration in Ethanol−Water Mixtures Using a Polarizable Force Field. *J. Phys. Chem. B* **2005**, *109*, 6705−13.
(22) Lamoureux, G.; Faraldo-Gomez, J.; Krupin, S. V.; S.Yu., N. A Novel Polarizable Model of Chloroform Based on Classical Drude Oscillators. *Chem. Phys. Lett.* **2009**, *268*, 270−274.
(23) Vorobyov, I.; Bennett, W. F. D.; Tieleman, D. P.; Allen, T. W.; Noskov, S. Y. The Role of Atomic Polarization in the Thermodynamics of Chloroform Partitioning to Lipid Bilayers. *J. Chem. Theory Comput.* **2012**, *8*, 618−628.
(24) Lamoureux, G.; Roux, B. Absolute Hydration Free Energy Scale for Alkali and Halide Ions Established from Simulations with a Polarizable Force Field. *J. Phys. Chem. B* **2006**, *110*, 3308−3322.
(25) Yu, H.; Mazzanti, C. L.; Whitfield, T. W.; Koeppe, R. E.; Andersen, O. S.; Roux, B. A Combined Experimental and Theoretical Study of Ion Solvation in Liquid N-Methylacetamide. *J. Am. Chem. Soc.* **2010**, *132*, 10847−10856.
(26) Kuhne, T. D.; Krack, M.; Mohamed, F. R.; Parrinello, M. Efficient and Accurate Car−Parrinello-like Approach to Born−Oppenheimer Molecular Dynamics. *Phys. Rev. Lett.* **2007**, *98*, 066401.
(27) Schlegel, H. B.; Iyengar, S. S.; Li, X.; Milliam, J. M.; Voth, G. A.; Scuseria, G. E.; Frisch, M. J. Ab Initio Molecular Dynamics: Propagating the Density Matrix with Gaussian Orbitals. III. Comparison with Born−Oppenheimer Dynamics. *J. Chem. Phys.* **2002**, *117*, 8694−8703.
(28) Ramaniah, L.; Bernasconi, M.; Parrinello, M. Ab Initio Molecular-Dynamics Simulation of K+ Solvation in Water. *J. Chem. Phys.* **1999**, *111*, 1587−1592.
(29) White, J.; Schwegler, E.; Galli, G.; Gygi, F. The Solvation of Na+ in Water: First-Principles Simulations. *J. Chem. Phys.* **2000**, *113*, 4668−4674.
(30) Rempe, S.; Pratt, L. The Hydration Number of Na+ in Liquid Water. *Fluid. Phas. Equil.* **2001**, *183*, 121−132.
(31) Rempe, S.; Asthagiri, D.; Pratt, L. Inner Shell Definition and Absolute Hydration Free Energy of K+(aq) on the Basis of Quasi-chemical Theory and Ab Initio Molecular Dynamics. *Phys. Chem. Chem. Phys.* **2004**, *6*, 1966−1969.
(32) Liu, Y.; Lu, H.; Wu, Y.; Hu, T.; Li, Q. Hydration and Coordination of K+ Solvation in Water from Ab Initio Molecular-Dynamics Simulation. *J. Chem. Phys.* **2010**, *132*, 124503.
(33) Azam, S. S.; Hofer, T. S.; Randolf, B. R.; Rode, B. M. Hydration of Sodium(I) and Potassium(I) Revisited: A Comparative QM/MM and QMCF MD Simulation Study of Weakly Hydrated Ions. *J. Phys. Chem. A* **2009**, *113*, 1827−1834.
(34) Rode, B.; Hofer, T.; Randolf, B.; Schwenk, C.; Xenides, D.; Vchirawongkwin, V. Ab Initio Quantum Mechanical Charge Field (QMCF) Molecular Dynamics: A QM/MM MD Procedure for Accurate Simulations of Ions and Complexes. *Theor. Chem. Acc.* **2006**, *115*, 77−85.
(35) D'Angelo, P.; Migliorati, V.; Guidoni, L. Hydration Properties of the Bromide Aqua Ion: The Interplay of First Principle and Classical Molecular Dynamics, and X-ray Absorption Spectroscopy. *Inorg. Chem.* **2010**, *49*, 4224−4231.
(36) Leung, K.; Rempe, S. B.; von Lilienfeld, O. A. Ab Initio Molecular Dynamics Calculations of Ion Hydration Free Energies. *J. Chem. Phys.* **2009**, *130*, 204507−204511.
(37) Kirchner, B.; di Dio, P. J.; Hutter, J. Real-World Predictions from Ab Initio Molecular Dynamics Simulations. *Top. Curr. Chem.* **2012**, *307*, 109−153.
(38) Nibbering, E. T.; Elsaesser, T. Ultrafast Vibrational Dynamics of Hydrogen Bonds in the Condensed Phase. *Chem. Rev.* **2004**, *104*, 1887−914.
(39) Marx, D.; Chandra, A.; Tuckerman, M. E. Aqueous Basic Solutions: Hydroxide Solvation, Structural Diffusion, and Comparison to the Hydrated Proton. *Chem. Rev.* **2010**, *110*, 2174−216.
(40) Warshel, A.; Sharma, P. K.; Kato, M.; Xiang, Y.; Liu, H. B.; Olsson, M. H. M. Electrostatic Basis for Enzyme Reaction. *Chem. Rev.* **2006**, *106*, 3210−3235.
(41) Warshel, A. Computer Simulations of Enzyme Catalysis: Methods, Progress, and Insights. *Ann. Rev. Biophys. Biomolec. Struct.* **2003**, *32*, 425−443.
(42) Heuft, J. M.; Meijer, E. J. Density Functional Theory Based Molecular-Dynamics Study of Aqueous Chloride Solvation. *J. Chem. Phys.* **2003**, *119*, 11788−11791.
(43) Riccardi, D.; Schaefer, P.; Yang, Y.; Yu, H. B.; Ghosh, P.; Prat-Resina, X.; Konig, P.; Li, G. H.; Xu, D. G.; Guo, H.; Elstner, M.; Cui, Q. C. Development of Effective Quantum Mechanical/Molecular Mechanical (QM/MM) Methods for Complex Biological Processes. *J. Phys. Chem. B* **2006**, *110*, 6458−6469.
(44) Bathelt, C. M.; Mulholland, A. J.; Harvey, J. N. QM/MM Modeling of Benzene Hydroxulation in Human Cytochrome P450 2C9. *J. Phys. Chem. B* **2008**, *112*, 13149−13156.
(45) Rod, T. H.; Ryde, U. Accurate QM/MM Free Energy Calculations of Enzyme Reactions: Methylation by Catechol o-Methyltransferase. *J. Chem. Theory Comput.* **2005**, *1*, 1240−1251.
(46) Hu, H.; Yang, W. Free Energies of Chemical Reactions in Solution and in Enzymes with Ab Initio Quantum Mechanics/Molecular Mechanics Methods. *Annu. Rev. Phys. Chem.* **2008**, *59*, 573−601.

(47) Kamerlin, S. C. L.; Haranczyk, M.; Warshel, A. Progress in Ab Initio QM/MM Free Energy Simulations of pK_a, Redox Reactions, and Solvation Free Energies. *J. Phys. Chem. B* **2009**, *113*, 1253−1272.
(48) Woodcock, H. L.; Hodoscek, M.; Sherwood, P.; Lee, Y. S.; Schaefer, H. F.; Brooks, B. R. Exploring the Quantum Mechanical/Molecular Mechanical Replica Path Method: A Pathway Optimization of the Chorismate to Prephenate Claisen Rearrangement Catalyzed by Chorismate Mutase. *Theor. Chem. Acc.* **2009**, *109*, 140−148.
(49) Woodcock, H. L.; Hodošček, M.; Gilbert, A. T. B.; Gill, P. M. W.; Schaefer, H. F.; Brooks, B. R. Interfacing Q-Chem and CHARMM to perform QM/MM reaction path calculations. *J. Comput. Chem.* **2007**, *28*, 1485−1502.
(50) Kästner, J.; Senn, H. M.; Thiel, S.; Otte, S.; Thiel, W. QM/MM Free-Energy Perturbation Compared to Thermodynamic Integration and Umbrella Sampling: Application to an Enzymatic Reaction. *J. Chem. Theor. Comp.* **2006**, *2*, 452−461.
(51) Senn, H. M.; Thiel, W. QM/MM Methods for Biomolecular Systems. *Angew. Chem. Intl. Ed.* **2009**, *48*, 1198−1229.
(52) Rowley, C. N.; Roux, B. The Solvation Structure of Na+ and K+ in Liquid Water Determined from High Level Ab Initio Molecular Dynamics Simulations. *J. Chem. Theory Comput.* **2012**, *8*, 3526−3535.
(53) Zhang, R.; Lev, B.; Cuervo, J. E.; Noskov, S. Y.; Salahub, D. R. A Guide to QM/MM Methodology and Applications. *Adv. Quantum Chem.* **2010**, *59*, 353−400.
(54) Lonsdale, R.; Harvey, J. N.; Mullholland, A. J. A Practical Guide to Modelling Enzyme-Catalyzed Reactions. *Chem. Soc. Rev.* **2012**, *41*, 3025−3038.
(55) Vreven, T.; Frisch, M. J.; Kudin, K. N.; Schlegel, H. B.; Morokuma, K. Geometry Optimization with QM/MM Methods II: Explicit Quadratic Coupling. *Mol. Phys.* **2006**, *104*, 701−714.
(56) Pentikainen, U.; Shaw, K. E.; Senthilkumar, K.; Woods, C. J.; Mulholland, A. J. Lennard-Jones Parameters for B3LYP/CHARMM27 QM/MM Modeling of Nucleic Acid Bases. *J. Chem. Theor. Comp.* **2009**, *5*, 396−410.
(57) Shaw, K. E.; Woods, C. J.; Mulholland, A. J. Compatibility of Quantum Chemical Methods and Empirical (MM) Water Models in Quantum Mechanics/Molecular Mechanics Liquid Water Simulations. *J. Phys. Chem. Lett.* **2010**, *1*, 219−223.
(58) Lev, B.; Zhang, R.; De la Lande, A.; Salahub, D.; Noskov, S. Y. The QM-MM Interface for CHARMM-deMon. *J. Comput. Chem.* **2010**, *31*, 1015−1023.
(59) Das, D.; Eurenius, K. P.; Billings, E. M.; Sherwood, P.; Chatfield, D. C.; Hodoscek, M.; Brooks, B. R. Optimization of Quantum Mechanical Molecular Mechanical Partitioning Schemes: Gaussian Delocalization of Molecular Mechanical Charges and the Double Link Atom Method. *J. Chem. Phys.* **2002**, *117*, 10534−10547.
(60) Faraldo-Gomez, J. D.; Roux, B. Characterization of Conformational Equilibria through Hamiltonian and Temperature Replica-Exchange Simulations: Assessing Entropic and Environmental Effects. *J. Comput. Chem.* **2007**, *28*, 1634−1647.
(61) Riahi, S.; Rowley, C. N.; Roux, B. QM/MM Molecular Dynamics Simulations of the Hydration of Mg(II) and Zn(II) Ions. *Can. J. Chem.* **2013**, *91*, 552−558.
(62) Beglov, D.; Roux, B. Finite Representation of an Infinite Bulk System—Solvent Boundary Potential for Computer Simulations. *J. Chem. Phys.* **1994**, *100*, 9050−9063.
(63) Tissandier, M. D.; Cowen, K. A.; Feng, W. Y.; Gundlach, E.; Cohen, M. H.; Earhart, A. D.; Tuttle, T. R.; Coe, J. V. The Proton'S Absolute Aqueous Enthalpy and Gibbs Free Energy of Solvation from Cluster Ion Solvation Data. *J. Phys. Chem. A* **1998**, *102*, 7791−7798.
(64) Gomer, R.; Tryson, G. Experimental-Determination of Absolute Half-Cell Emfs and Single Ion Free-Energies of Solvation. *J. Chem. Phys.* **1977**, *66*, 4413−4424.
(65) Schmid, R.; Miah, A. M.; Sapunov, V. N. A New Table of the Thermodynamic Quantities of Ionic Hydration: Values and Some Applications (Enthalpy−Entropy Compensation and Born Radii). *Phys. Chem. Chem. Phys.* **2000**, *2*, 97−102.
(66) Klots, C. E. Solubility of Protons in Water. *J. Phys. Chem.* **1981**, *85*, 3585−3588.
(67) Ponder, J. W.; Wu, C. J.; Ren, P. Y.; Pande, V. S.; Chodera, J. D.; Schnieders, M. J.; Haque, I.; Mobley, D. L.; Lambrecht, D. S.; DiStasio, R. A.; Head-Gordon, M.; Clark, G. N. I.; Johnson, M. E.; Head-Gordon, T. Current Status of the AMOEBA Polarizable Force Field. *J. Phys. Chem. B* **2010**, *114*, 2549−2564.
(68) Joung, I. S.; Cheatham, T. E. Determination of Alkali and Halide Monovalent Ion Parameters for Use in Explicitly Solvated Biomolecular Simulations. *J. Phys. Chem. B* **2008**, *112*, 9020−9041.
(69) Bankura, A.; Carnevale, V.; Klein, M. L. Hydration Structure of Salt Solutions from Ab Initio Molecular Dynamics. *J. Chem. Phys.* **2013**, *138*, 014501.
(70) Skipper, N. T.; Neilson, G. W. X-Ray and Neutron-Diffraction Studies on Concentrated Aqueous-Solutions of Sodium-Nitrate and Silver-Nitrate. *J. Phys. Cond. Matt.* **1989**, *1*, 4141−4154.
(71) Mähler, J.; Persson, I. A Study of the Hydration of the Alkali Metal Ions in Aqueous Solution. *Inorg. Chem.* **2012**, *51*, 425−438.
(72) Glezakou, V.-A.; Chen, Y.; Fulton, J.; Schenter, G.; Dang, L. Electronic Structure, Statistical Mechanical Simulations, and EXAFS Spectroscopy of Aqueous Potassium. *Theor. Chem. Acc.* **2006**, *115*, 86−99.
(73) Soper, A. K.; Weckström, K. Ion Solvation and Water Structure in Potassium Halide Aqueous Solutions. *Biophys. Chem.* **2006**, *124*, 180−191.
(74) Tongraar, A.; Rode, B. M. The Hydration Structures of F and Cl Investigated by Ab Initio QM/MM Molecular Dynamics Simulations. *Phys. Chem. Chem. Phys.* **2003**, *5*, 357−362.
(75) Bergstrom, P. A.; Lindgren, J.; Kristiansson, O. An IR Study of the Hydration of ClO_4^-, NO_3^-, I^-, Br^-, Cl^-, and SO_4^{2-} Anions in Aqueous Solution. *J. Phys. Chem.* **1991**, *95*, 8575−8580.
(76) D'Angelo, P.; Dinola, A.; Filipponi, A.; Pavel, N. V.; Roccatano, D. An Extended X-Ray-Absorption Fine-Structure Study of Aqueous-Solutions by Employing Molecular-Dynamics Simulations. *J. Chem. Phys.* **1994**, *100*, 985−994.
(77) Wallen, S. L.; Palmer, B. J.; Pfund, D. M.; Fulton, J. L.; Newville, M.; Ma, Y. J.; Stern, E. A. Hydration of Bromide Ion in Supercritical Water: An X-ray Absorption Fine Structure and Molecular Dynamics Study. *J. Phys. Chem. A* **1997**, *101*, 9632−9640.
(78) Beudert, R.; Bertagnolli, H.; Zeller, M. Ion−Ion and Ion−Water Interactions in an Aqueous Solution of Erbium Bromide (ErBr3). A Differential Anomalous X-ray Scattering Study. *J. Chem. Phys.* **1997**, *106*, 8841−8848.
(79) Raugei, S.; Klein, M. L. An Ab Initio Study of Water Molecules in the Bromide Ion Solvation Shell. *J. Chem. Phys.* **2002**, *116*, 196−202.